

---

# Learning to Infer Graphics Programs from Hand-Drawn Images

---

Anonymous Author(s)

Affiliation

Address

email

## Abstract

1 We introduce a model that learns to convert simple hand drawings into graphics  
2 programs written in a subset of  $\text{\LaTeX}$ . The model combines techniques from deep  
3 learning and program synthesis. We learn a convolutional neural network that  
4 proposes plausible drawing primitives that explain an image. This set of drawing  
5 primitives is like an execution trace for a graphics program. From this trace we use  
6 program synthesis techniques to recover a graphics program with constructs like  
7 variable bindings, iterative loops, or simple kinds of conditionals. With a graphics  
8 program in hand, we can correct errors made by the deep network, cluster drawings  
9 by use of similar high-level geometric structures, and extrapolate drawings. Taken  
10 together these results are a step towards agents that induce useful, human-readable  
11 programs from perceptual input.

## 12 1 Introduction

13 How can an agent convert noisy, high-dimensional perceptual input to a symbolic, abstract object, such  
14 as a computer program? Here we consider this problem within a graphics program synthesis domain.  
15 We develop an approach for converting natural images, such as hand drawings, into executable source  
16 code for drawing the original image. The graphics programs in our domain draw simple figures like  
17 those found in machine learning papers (see Figure 1a).

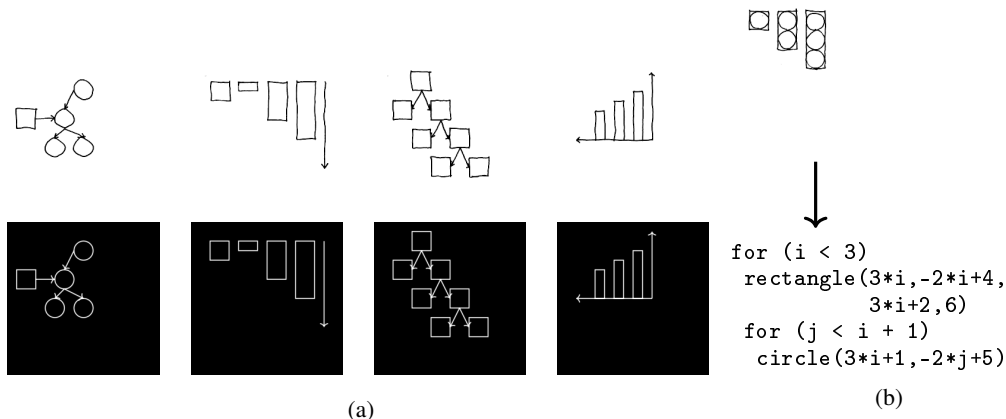


Figure 1: (a): Model learns to convert hand drawings (top) into  $\text{\LaTeX}$  (bottom). (b) Synthesizes high-level *graphics program* from hand drawing.

18 The key observation behind our work is that generating a programmatic representation from an image  
19 of a diagram actually involves two distinct steps that require different technical approaches. The first  
20 step involves identifying the components such as rectangles, lines and arrows that make up the image.  
21 The second step involves identifying the high-level structure in how the components were drawn. In  
22 Figure 1(b), it means identifying a pattern in how the circles and rectangles are being drawn that is  
23 best described with two nested loops, and which can easily be extrapolated to a bigger diagram.

24 We present a hybrid architecture for inferring graphics programs that is structured around these  
25 two steps. For the first step, our approach uses a deep network to infer a sequence of primitive  
26 shape-drawing commands that can generate an image similar to the observed image. We refer to this  
27 sequence as a *execution trace*, since it corresponds to the sequence of primitive commands that a  
28 program would have issued, but it lacks the high-level structure that determines how the program  
29 decided to issue those commands. For added robustness, we train the network to produce a proposal  
30 distribution of the most likely traces, and use stochastic search to find the trace that best matches the  
31 input. The network is trained from an automatically generated corpus of synthetic image generating  
32 programs.

33 The second step involves generating a high-level program capable of producing the program trace  
34 identified by the first phase. This paper argues that this stage is best achieved by *constraint-based*  
35 *program synthesis* [1]. Without the need for training, the program synthesizer can search the space of  
36 possible programs for one capable of producing the desired trace.

## 37 2 Related work

38 Our work bears resemblance to the Attend-Infer-Repeat (AIR) system, which learns to decompose an  
39 image into its constituent objects [3]. AIR learns an iterative inference scheme which infers objects  
40 one by one and also decides when to stop inference; this is similar to our approach’s first stage, which  
41 parses images into program execution traces. Our approach further produces interpretable, symbolic  
42 programs which generate those execution traces. The two approaches also differ in their architectures  
43 and training regimes: AIR learns a recurrent auto-encoding model via variational inference, whereas  
44 our parsing stage learns an autoregressive-style model from randomly-generated (execution trace,  
45 image) pairs. Finally, while AIR was evaluated on multi-MNIST images and synthetic 3D scenes, we  
46 focus on hand-drawn sketches.

47 Our image-to-execution-trace parsing architecture builds on prior work on controlling procedural  
48 graphics programs [4]. Given a program which generates random 2D recursive structures such as  
49 vines, that system learns a structurally-identical “guide program” whose output can be directed, via  
50 neural networks, to resemble a given target image. We adapt this method to a different visual domain  
51 (figures composed of multiple objects), using a broad prior over possible scenes as the initial program  
52 and viewing the execution trace through the guide program as a symbolic parse of the target image.  
53 We then show how to synthesize higher-level programs from these execution traces.

54 In the computer graphics literature, there have been other systems which convert sketches into  
55 procedural representations. One uses a convolutional network to match a sketch to the output of a  
56 parametric 3D modeling system [5]. Another uses convolutional networks to support sketch-based  
57 instantiation of procedural primitives within an interactive architectural modeling system [6]. Both  
58 systems focus on inferring fixed-dimensional parameter vectors. In contrast, we seek to automatically  
59 infer a structured, programmatic representation of a sketch which captures higher-level visual patterns.

60 Prior work has also applied sketch-based program synthesis to authoring graphics programs. Sketch-  
61 n-Sketch is a bi-directional editing system in which direct manipulations to a program’s output  
62 automatically propagate to the program source code [7]. We see this work as complementary to our  
63 own: programs produced by our method could be provided to a Sketch-n-Sketch-like system as a  
64 starting point for further editing.

65 The CogSketch [8] system also aims to have a high-level understanding of hand-drawn figures.  
66 Their primary goal is cognitive modeling (eg, they apply their system to solving IQ-test style visual  
67 reasoning problems), whereas we are interested in building an automated AI application (eg, in our  
68 system the user need not annotate which strokes correspond to which shapes; our neural network  
69 produces something equivalent to the annotations). A key similarity however is that both CogSketch  
70 and our system have as a goal to make it easier to produce nice-looking figures. Unsupervised Program

71 Synthesis [9] is a related framework which was also applied to geometric reasoning problems. The  
 72 goals of [9] were cognitive modeling, and they applied their technique to synthetic scenes used in  
 73 human behavioral studies.

### 74 3 Neural architecture for inferring drawing execution traces

75 We developed a deep network architecture for efficiently inferring a execution trace,  $T$ , from an  
 76 image,  $I$ . Our model constructs the trace one drawing command at a time. When predicting the next  
 77 drawing command, the network takes as input the target image  $I$  as well as the rendered output of  
 78 previous drawing commands. Intuitively, the network looks at the image it wants to explain, as well  
 79 as what it has already drawn. It then decides either to stop drawing or proposes another drawing  
 80 command to add to the execution trace; if it decides to continue drawing, the predicted primitive is  
 81 rendered to its “canvas” and the process repeats.

82 Figure 2 illustrates this architecture. We first pass a  $256 \times 256$  target image and a rendering of the  
 83 trace so far (encoded as a two-channel image) to a convolutional network. Given the features extracted  
 84 by the convnet, a multilayer perceptron then predicts a distribution over the next drawing command  
 85 to add to the trace; see Table 1. We predict the drawing command token-by-token, conditioning  
 86 each token both on the image features and on the previously generated tokens. For example, the  
 87 network first decides to emit the `circle` token conditioned on the image features, then it emits the  
 88  $x$  coordinate of the circle conditioned on the image features and the `circle` token, and finally it  
 89 predicts the  $y$  coordinate of the circle conditioned on the image features, the `circle` token, and  
 90 the  $x$  coordinate. See supplement for the full details of the architecture, which we implemented in  
 91 Tensorflow [10]. The distribution over the next drawing command factorizes as:

$$\mathbb{P}_{\theta}[t_1 t_2 \cdots t_K | I, T] = \prod_{k=1}^K \mathbb{P}_{\theta}[t_k | f_{\theta}(I, \text{render}(T)), \{t_j\}_{j=1}^{k-1}] \quad (1)$$

92 where  $t_1 t_2 \cdots t_K$  are the tokens in the drawing command,  $I$  is the target image,  $T$  is an execution trace,  
 93  $\theta$  are the parameters of the neural network, and  $f_{\theta}(\cdot, \cdot)$  is the image feature extractor (convolutional  
 94 network). The distribution over execution traces factorizes as:

$$\mathbb{P}_{\theta}[T | I] = \prod_{n=1}^{|T|} \mathbb{P}_{\theta}[T_n | I, T_{1:(n-1)}] \times \mathbb{P}_{\theta}[\text{STOP} | I, T] \quad (2)$$

95 where  $|T|$  is the length of execution trace  $T$ , the subscripts on  $T$  index drawing commands within the  
 96 trace, and the `STOP` token is emitted by the network to signal that the trace explains the image.

97 We train the network by sampling execution traces  $T$  and target images  $I$  for randomly generated  
 98 scenes and maximizing (2) with respect to  $\theta$  by gradient ascent. Training does not require back-  
 99 propagation across the entire sequence of drawing commands: drawing to the canvas ‘blocks’ the  
 100 gradients, effectively offloading memory to an external visual store. In a sense, this model is like an  
 101 autoregressive variant of AIR [3] without attention. We trained the network on  $10^5$  scenes, which  
 102 takes a little less than a day on an Nvidia TitanX GPU.

<code>circle</code> ( $x, y$ )	Circle at $(x, y)$
<code>rectangle</code> ( $x_1, y_1, x_2, y_2$ )	Rectangle with corners at $(x_1, y_1)$ & $(x_2, y_2)$
<code>line</code> ( $x_1, y_1, x_2, y_2$ , $\text{arrow} \in \{0, 1\}, \text{dashed} \in \{0, 1\}$ )	Line from $(x_1, y_1)$ to $(x_2, y_2)$ , optionally with an arrow and/or dashed
<code>STOP</code>	Finishes execution trace inference

Table 1: The deep network in (2) predicts drawing commands, shown above.

103 This network suffices to “derender” synthetic images like those shown in Figure 3. We can perform a  
 104 beam search decoding to recover what the network thinks is the most likely execution trace for images  
 105 like these, recovering traces maximizing  $\mathbb{P}_{\theta}[T | I]$ . But, if the network makes a mistake (predicts an  
 106 incorrect line of code), it has no way of recovering from the error. In order to derender an image  
 107 with  $n$  objects, it must correctly predict  $n$  drawing commands – so its probability of success will  
 108 decrease exponentially in  $n$ , assuming it has any nonzero chance of making a mistake. For added

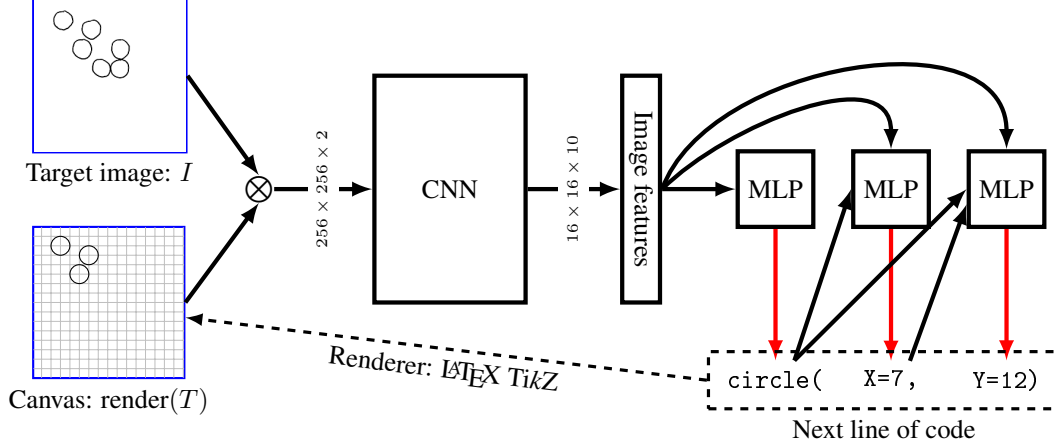


Figure 2: Our neural architecture for inferring the execution trace of a graphics program from its output. **Blue**: network inputs. **Black**: network operations. **Red**: samples from a multinomial. Typewriter font: network outputs. Renders snapped to a  $16 \times 16$  grid, illustrated in gray.

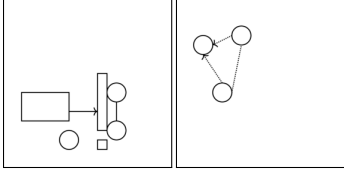


Figure 3: Network is trained to infer execution traces for randomly generated scenes like the two shown above. See supplement for details of the training data generation.

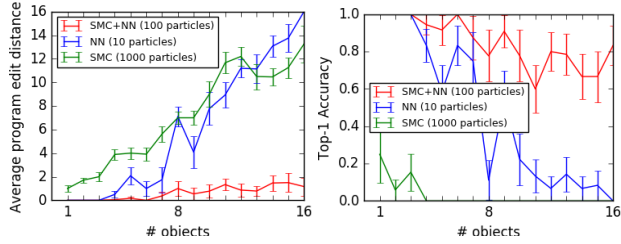


Figure 4: Using the model to parse latex output. The model is trained on diagrams with up to 8 objects. As shown above it generalizes to scenes with many more objects. Neither the stochastic search nor the neural network are sufficient on their own. # particles varies by model: we compare the models *with equal runtime* ( $\approx 1$  sec/object)

robustness as  $n$  becomes large, we treat the neural network outputs as proposals for a Sequential Monte Carlo (SMC) sampling scheme [11]. For the SMC sampler, we use pixel-wise distance as a surrogate for a likelihood function. The SMC sampler is designed to produce samples from the distribution  $\propto L(I|\text{render}(T))\mathbb{P}_\theta[T|I]$ , where  $L(\cdot|\cdot) : \text{image}^2 \rightarrow \mathcal{R}$  uses the distance between two images as a proxy for a likelihood. Figure 4 compares the neural network with SMC against the neural network by itself or SMC by itself. Only the combination of the two passes a critical test of generalization: when trained on images with  $\leq 8$  objects, it successfully parses scenes with many more objects than the training data.

### 3.1 Generalizing to hand drawings

A practical application of our neural network is the automatic conversion of hand drawings into a subset of  $\text{\LaTeX}$ . We train the model to generalize to hand drawings by introducing noise into the renderings of the training target images. We designed this noise process to introduce the kinds of variations found in hand drawings (Figure 5; see supplement for details). Our neurally-guided SMC procedure used pixel-wise distance as a surrogate for a likelihood function ( $L(\cdot|\cdot)$  in section 3). But pixel-wise distance fares poorly on hand drawings, which never exactly match the model’s renders. So, for hand drawings, we *learn* a surrogate likelihood function,  $L_{\text{learned}}(\cdot|\cdot)$ . The density  $L_{\text{learned}}(\cdot|\cdot)$  is predicted by a convolutional network that we train to predict the distance between two traces conditioned upon their renderings. We train our likelihood surrogate to approximate the symmetric difference, which is the number of drawing commands by which two traces differ:

$$-\log L_{\text{learned}}(\text{render}(T_1)|\text{render}(T_2)) \approx |T_1 - T_2| + |T_2 - T_1| \quad (3)$$

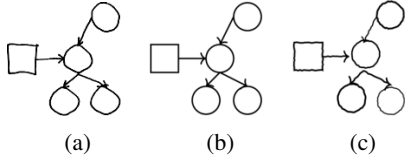


Figure 5: (a): a hand drawing. (b): Rendering of the trace our model infers for (a). We can generalize to hand drawings like these because we train the model on images corrupted by a noise process designed to resemble the kind of noise introduced by hand drawings - see (c) for a noisy rendering of (b).

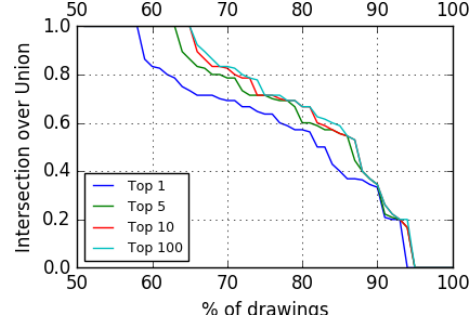


Figure 6: How close are the model’s outputs to the ground truth on hand drawings, as we consider larger sets of samples (1,5,10,100)? Distance to ground truth trace measured by the intersection over union of predicted vs. ground truth traces (sets of drawing commands).

Intuitively, Eq. 3 says that  $L_{\text{learned}}(\cdot|\cdot)$  approximates the distance between the trace we want and the trace we have so far. Pixel-wise distance metrics are sensitive to the details of how arrows, dashes, and corners are drawn – but we wish to be invariant to these details. So, we learn a distance metric over images that approximates the distance metric in the search space over traces.

We drew 100 figures by hand; see figure 7. These were drawn carefully but not perfectly. Our model assumes that objects are snapped to a  $16 \times 16$  grid, so we made the drawings on graph paper.

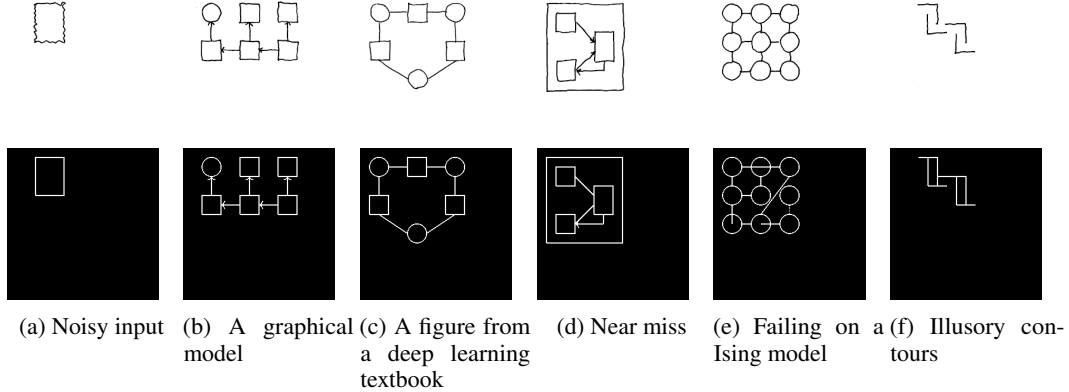


Figure 7: Example drawings above model outputs. See also Fig. 1. Stochastic search (SMC) can help correct for these errors, as can the program synthesizer (Section 4.1)

For each drawing we annotated a ground truth trace, and evaluated the model by asking it to sample many candidate traces for each drawing. For 58% of the drawings the Top-1 most likely sample exactly matches the ground truth; as we consider more samples the model encounters traces that are closer to the ground truth annotation (Fig. 6). Because our current model sometimes makes mistakes, we envision it working as follows: a user sketches a diagram, and the system responds by proposing a few candidate interpretations. The user could then select one and edit it if necessary.

## 4 Synthesizing graphics programs from execution traces

Although the execution trace of a graphics program describes the parts of a scene, it fails to encode higher-level features of the image, such as repeated motifs or symmetries. A *graphics program* better describe structures like these, and we now take as our goal to synthesize simple graphics programs from their execution traces.

145 We constrain the space of allowed programs by writing down a context free grammar over a space of  
 146 programs. Although it might be desirable to synthesize programs in a Turing-complete language such  
 147 as Lisp or Python, a more tractable approach is to specify what in the program languages community  
 148 is called a Domain Specific Language (DSL) [12]. Our DSL (Table 2) encodes prior knowledge of  
 149 what graphics programs tend to look like.

---

Program	→	Command; ...; Command
Command	→	circle(Expression, Expression)
Command	→	rectangle(Expression, Expression, Expression, Expression)
Command	→	line(Expression, Expression, Expression, Expression, Boolean, Boolean)
Command	→	for( $0 \leq \text{Var} < \text{Expression}$ ) { if ( $\text{Var} > 0$ ) { Program }; Program }
Command	→	reflect(Axis) { Program }
Expression	→	$\mathcal{Z} * \text{Var} + \mathcal{Z}$
Var	→	A free (unused) variable
$\mathcal{Z}$	→	an integer
Axis	→	$X = \mathcal{Z} \mid Y = \mathcal{Z}$

---

Table 2: Grammar over graphics programs. We allow loops (for) with conditionals (if), vertical/horizontal reflections (reflect), variables (Var) and affine transformations ( $\mathcal{Z} * \text{Var} + \mathcal{Z}$ ).

150 Given the DSL and a trace  $T$ , we want to recover a program that both evaluates to  $T$  and, at the same  
 151 time, is the “best” explanation of  $T$ . For example, we might prefer more general programs or, in the  
 152 spirit of Occam’s razor, prefer shorter programs. We wrap these intuitions up into a cost function  
 153 over programs, and seek the minimum cost program consistent with  $T$ :

$$\text{program}(T) = \arg \min_{p \in \text{DSL, s.t. } p \text{ evaluates to } T} \text{cost}(p) \quad (4)$$

154 We define the cost of a program to be the number of statements it contains, where a statement is a  
 155 “Command” in Table 2. We also penalize using many different numerical constants; see supplement.

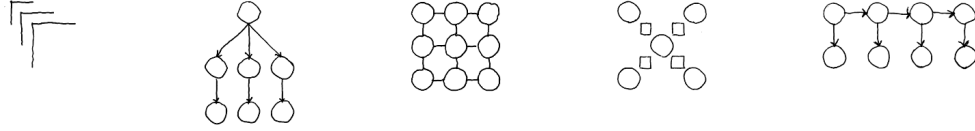
156 The constrained optimization problem in equation 4 is intractable in general, but there exist efficient-  
 157 in-practice tools for finding exact solutions to program synthesis problems like these. We use the  
 158 state-of-the-art Sketch tool [1]. Describing Sketch’s program synthesis algorithm is beyond the  
 159 scope of this paper; see [1]. At a high level, Sketch takes as input a space of programs, along with  
 160 a specification of the program’s behavior and optionally a cost function. It translates the synthesis  
 161 problem into a constraint satisfaction problem, and then uses a SAT solver to find a minimum cost  
 162 program satisfying the specification. In exchange for not having any guarantees on how long it will  
 163 take to find a minimum cost solution, it comes with the guarantee that it will always find a globally  
 164 optimal program.

165 Why synthesize a graphics program, if the execution trace already suffices to recover the objects in  
 166 an image? Within our domain of hand-drawn figures, graphics program synthesis has several uses:

#### 167 4.1 Correcting errors made by the neural network

168 The program synthesizer can help correct errors from the execution trace proposal network by favoring  
 169 execution traces which lead to more concise or general programs. For example, one generally prefers  
 170 figures with perfectly aligned objects over figures whose parts are slightly misaligned – and precise  
 171 alignment lends itself to short programs. Concretely, we estimated a prior over programs. Then,  
 172 given the few most likely traces output by the neurally guided sampler, we reranked them according  
 173 to the prior probability of their programs. Our neurally guided sampler could only do better on 7  
 174 drawings by looking at the Top-100 sampled traces (see Fig. 6), precluding a statistically significant  
 175 analysis of how much learning a prior over programs could help correct errors. But, learning this prior  
 176 does sometimes help correct mistakes made by the neural network, and also occasionally introduces  
 177 mistakes of its own; see Fig. 9 for a representative example of the kinds of corrections that it makes.  
 178 See supplement for details.

#### 179 4.2 Modeling similarity between drawings



```

for(i<3){
  line(i,-1*i+6,
2*i+2,-1*i+6)
  line(i,-2*i+4,
i,-1*i+6)
}

circle(4,10)
for(i<3){
  circle(-3*i+7,5)
  circle(-3*i+7,1)
  line(-3*i+7,4,
-3*i+7,2,
  arrow=True)
  line(4,9,
-3*i+7,6,
  arrow=True)
}

for(i<3)
  for(j<3)
    if(j>0)
      line(-3*j+8,
-3*i+7,-3*j+9,
-3*i+7)
      line(-3*i+7,-3*j+8,
3*i+1)
      circle(3*i+1,
3*i+1)
      circle(-3*j+7,-3*i+7)
}

reflect(y=8){
  for(i<3){
    for(j<3){
      if(i>0){
        rectangle(3*i-1,
2,3*i,3)}
        circle(3*i+1,
3*i+1)
      }
    }
  }
}

for(i<4){
  line(-4*i+13,4,
-4*i+13,2,
  arrow=True)
  for(j<3){
    if(j>0){
      circle(-4*i+13,
4*j+-3)}
      line(-4*j+10,5,
-4*j+12,5,
  arrow=True)
    }
  }
}

```

Figure 8: Example drawings (top row) and the programs we synthesize from their ground truth traces (bottom row). Notice the nested loops in the Ising model (middle), special case conditionals for the HMM (rightmost), combination of symmetry and iteration in middle left, and affine transformation in the leftmost figure.

180 Modeling an image using a program opens up new ways of  
 181 measuring similarity between drawings. For example, we  
 182 might say that two drawings are similar if they both contain  
 183 repetitions of length 4, or if they share the same reflectional  
 184 symmetry, or if they are both organized according to a grid-  
 185 like structure.

186 We measure the similarity between two drawings by ex-  
 187 tracting features of the best programs that describe them.  
 188 Our features are counts of the number of times that dif-  
 189 ferent components in the DSL were used (Table 2). We  
 190 project these features down to a 2-dimensional subspace  
 191 using nonnegative matrix factorization (NMF: [13]); see  
 192 Fig.10. One could use many alternative similarity metrics  
 193 between drawings which would capture pixel-level while  
 194 missing high-level geometric similarities. We used our learned distance metric between execu-  
 195 tion traces,  $L_{\text{learned}}(\cdot|\cdot)$ , and projected to a 2-dimensional subspace using multidimensional scaling  
 196 (MDS: [14]). This reveals similarities between the objects in the drawings, while missing similarities  
 197 at the level of the program.

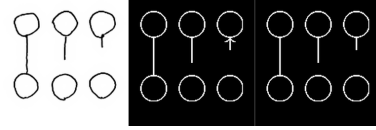


Figure 9: Left: hand drawing. Center: interpretation favored by the deep network. Right: interpretation favored after learning a prior over programs. Our learned prior favors shorter, simpler programs, thus continuing the pattern of not having an arrow is preferred.

### 198 4.3 Extrapolating figures

199 Having access to the source code of a graphics program facilitates coherent, high-level edits to the  
 200 figure generated by that program. For example, we can change all of the circles to squares or make all  
 201 of the lines dashed. We can also **extrapolate** figures by increasing the number of times that loops  
 202 are executed. Extrapolating repetitive visual patterns comes naturally to humans, and building this  
 203 ability into an application is practical: imagine hand drawing a repetitive graphical model structure  
 204 and having our system automatically induce and extend the pattern. Fig. 12 shows extrapolations of  
 205 programs synthesized from ground truth traces; see supplement for our full set of extrapolations.

## 206 5 Conclusion

207 We have presented a system for inferring graphics programs which generate  $\text{\LaTeX}$ -style figures from  
 208 hand-drawn images. The system uses a combination of deep neural networks and stochastic search to  
 209 parse drawings into symbolic execution traces; it then feeds these traces to a general-purpose program  
 210 synthesis engine to infer a structured graphics program. We evaluated our model’s performance at

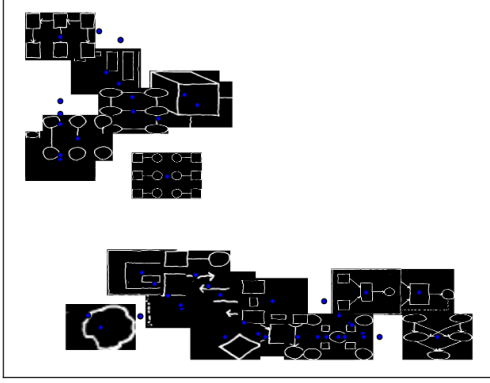


Figure 10: NMF on features of the programs that were synthesized for each image. Horizontal component roughly corresponds to “symmetry” while vertical component roughly corresponds to “loopyness”, with images on the diagonal having both of these.

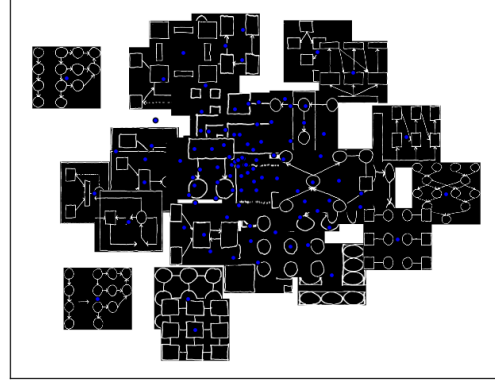


Figure 11: MDS on drawings using the learned distance metric,  $L_{\text{learned}}(\cdot|\cdot)$ . Drawings with similar looking parts in similar locations are clustered together.

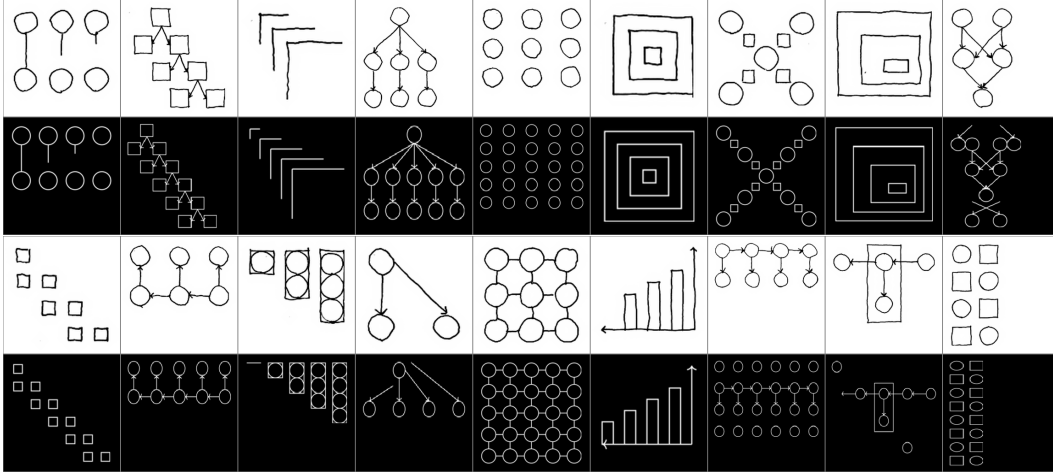


Figure 12: Top, white: hand drawings. Bottom, black: extrapolations produced by running loops for extra iterations.

211 parsing novel images, and we demonstrated its ability to extrapolate from provided drawings and to  
 212 organize them according to high-level geometric features.

213 There are many directions for future work. In the parsing phase, the proposal network currently  
 214 samples positional variables on a discrete grid. More general types of drawings could be supported  
 215 by instead sampling from continuous distributions, e.g. using Mixture Density Networks [15]. The  
 216 proposal network also currently handles only a very small subset of  $\text{\LaTeX}$  drawing commands, though  
 217 there is no reason that it could not be extended to handle more with a higher-capacity network.  
 218 Exploring more sophisticated network architectures, including ones that utilize attention [16], could  
 219 help correct some of the errors the network makes. In the synthesis phase, a more expressive DSL—  
 220 including subroutines, recursion, and symmetry groups beyond reflections—would allow the system  
 221 to effectively model a wider variety of graphical phenomena. The synthesizer itself could also be  
 222 the subject of future work: the system currently uses the general-purpose Sketch synthesizer, which  
 223 can take minutes to hours to run, whereas program synthesizers which are custom-built for special  
 224 problem domains can run much faster or even interactively [17].

225 In the not-too-distant future, we believe it should be possible to produce professional-looking figures  
 226 just by drawing them and then letting an artificially-intelligent agent write the code. More generally,



we believe that the two-phase system we have proposed—parsing into execution traces, then searching for a low-cost symbolic program which generates those traces—may be a useful paradigm for domains in which agents must programmatically reason about noisy perceptual input.

## References

- [1] Armando Solar Lezama. *Program Synthesis By Sketching*. PhD thesis, EECS Department, University of California, Berkeley, Dec 2008.
- [2] Leonardo De Moura and Nikolaj Bjørner. Z3: An efficient smt solver. In *Tools and Algorithms for the Construction and Analysis of Systems*, pages 337–340. Springer, 2008.
- [3] SM Eslami, N Heess, and T Weber. Attend, infer, repeat: Fast scene understanding with generative models. arxiv preprint arxiv:..., 2016. URL <http://arxiv.org/abs/1603.08575>.
- [4] Daniel Ritchie, Anna Thomas, Pat Hanrahan, and Noah Goodman. Neurally-guided procedural models: Amortized inference for procedural graphics programs using neural networks. In *Advances In Neural Information Processing Systems*, pages 622–630, 2016.
- [5] Haibin Huang, Evangelos Kalogerakis, Ersin Yumer, and Radomir Mech. Shape synthesis from sketches via procedural models and convolutional networks. *IEEE transactions on visualization and computer graphics*, 2017.
- [6] Gen Nishida, Ignacio Garcia-Dorado, Daniel G. Aliaga, Bedrich Benes, and Adrien Bousseau. Interactive sketching of urban procedural models. *ACM Trans. Graph.*, 35(4), 2016.
- [7] Brian Hempel and Ravi Chugh. Semi-automated svg programming via direct manipulation. In *Proceedings of the 29th Annual Symposium on User Interface Software and Technology*, UIST '16, pages 379–390, New York, NY, USA, 2016. ACM.
- [8] Kenneth Forbus, Jeffrey Usher, Andrew Lovett, Kate Lockwood, and Jon Wetzell. Cogsketch: Sketch understanding for cognitive science research and for education. *Topics in Cognitive Science*, 3(4):648–666, 2011.
- [9] Kevin Ellis, Armando Solar-Lezama, and Josh Tenenbaum. Unsupervised learning by program synthesis. In *Advances in Neural Information Processing Systems*, pages 973–981, 2015.
- [10] Martín Abadi, Ashish Agarwal, Paul Barham, Eugene Brevdo, Zhifeng Chen, Craig Citro, Greg S. Corrado, Andy Davis, Jeffrey Dean, Matthieu Devin, Sanjay Ghemawat, Ian Goodfellow, Andrew Harp, Geoffrey Irving, Michael Isard, Yangqing Jia, Rafal Jozefowicz, Lukasz Kaiser, Manjunath Kudlur, Josh Levenberg, Dan Mané, Rajat Monga, Sherry Moore, Derek Murray, Chris Olah, Mike Schuster, Jonathon Shlens, Benoit Steiner, Ilya Sutskever, Kunal Talwar, Paul Tucker, Vincent Vanhoucke, Vijay Vasudevan, Fernanda Viégas, Oriol Vinyals, Pete Warden, Martin Wattenberg, Martin Wicke, Yuan Yu, and Xiaoqiang Zheng. TensorFlow: Large-scale machine learning on heterogeneous systems, 2015. Software available from tensorflow.org.
- [11] Arnaud Doucet, Nando De Freitas, and Neil Gordon, editors. *Sequential Monte Carlo Methods in Practice*. Springer, 2001.
- [12] Oleksandr Polozov and Sumit Gulwani. Flashmeta: A framework for inductive program synthesis. *ACM SIGPLAN Notices*, 50(10):107–126, 2015.
- [13] Daniel D Lee and H Sebastian Seung. Learning the parts of objects by non-negative matrix factorization. *Nature*, 401(6755):788–791, 1999.
- [14] Michael AA Cox and Trevor F Cox. Multidimensional scaling. *Handbook of data visualization*, pages 315–347, 2008.
- [15] Christopher M. Bishop. Mixture Density Networks. Technical report, 1994.
- [16] Volodymyr Mnih, Nicolas Heess, Alex Graves, et al. Recurrent models of visual attention. In *Advances in neural information processing systems*, pages 2204–2212, 2014.
- [17] Vu Le and Sumit Gulwani. Flashextract: a framework for data extraction by examples. In *ACM SIGPLAN Notices*, volume 49, pages 542–553. ACM, 2014.